DOI: 10.1021/ma901927m

Macromolecules
NOTE

Fast Dynamics and Conformations of Polymer in a Conformational Disordered Crystal Characterized by $^{1}H-^{13}C$ WISE NMR

Toshikazu Miyoshi,*,† Al Mamun,† and Detlef Reichert‡

†*National Institute of Advanced Industrial Science and Technology, Research Institute of Nanotechnology, Tsukuba Central 5-1 1-1-1 Higashi, Tsukuba, Ibaraki 305-8565, Japan, and* ‡*University of Halle/Faculty of Science II Department of Physics/Biophysics Group, Betty-Heimann-Strasse 7, 06120 Halle, Germany*

Received August 31, 2009; Revised Manuscript Received January 25, 2010

Introduction

Many polymers with flexible side groups form conformationally disordered (CONDIS) crystals under ambient pressures.[1−3] Allegra et al. and Sozzani et al. pointed out that the flexibility of side groups plays an important role in the stability of these phases.[3,4] However, it is difficult to determine the conformation of the side group and their dynamics in the disordered phase. Moreover, the disordered phase induces a faster dynamics in the backbone than that in the crystalline phase.[5] Unraveling of the CONDIS nature of side-chain-containing polymer is necessary to understand not only their static structures but also complex dynamics in their backbone and the side groups.

Isotactic poly(1-butene) (*i*PB1) forms polymorphs and crystallizes as form II from the melt state, which spontaneously transforms into the stable form I at ambient temperature.[6] X-ray diffraction (XRD) analysis has shown that the form II consists of four 11_3 helices packed in a tetragonal lattice, but this method could not properly detect the conformations of the side chain.[7] Recently, Miyoshi et al. used ^{13}C high-resolution solid-state (SS) NMR to show that the side groups in form II adopt two conformations, *trans*−*gauche*′ and *gauche*′−*gauche*, with respect to the two carbons in γ-positions, and these conformations exhibit dynamic conformational transitions above 165 K.[8] The conformational analysis was based on the empirical γ gauche effect[9] and MM3 calculations.[10] Furthermore, it was shown by high-resolution SS-NMR that the overall motion in form II reaches a frequency of ∼50 kHz at temperatures slightly above ambient temperature.[11] Previous NMR results[8,11] have shown form II of *i*PB1 to be a dynamic CONDIS crystal; however, information on the detailed geometry of the backbone dynamics and conformational dynamics of the side chain has yet to be obtained. To gain information about the amplitude of high-frequency motions, experiments aimed to detect the values of anisotropic interaction parameters can be used. These interactions are partially averaged by fast but anisotropic molecular dynamics and can be analyzed quantitatively in terms of reorientational angles. Litvinov et al. for the first time analyzed the complex dynamics of poly(diethylsiloxane) (PDES) in crystals and mesophases by residual ^{2}H quadrupole interactions.[12] However, the application of ^{2}H NMR requires isotope labeling, as the natural abundance is too low to be used. In contrast, ^{1}H is an attractive nucleus because of its highest sensitivity among all the available nuclei; however, its high natural abundance and the large gyromagnetic ratio result in multispin interactions which severely complicate the quantitative interpretation of the dynamic NMR data.[13−16] So far, molecular dynamics of liquid crystals,[17] adamantane,[18] and substituted benzenes confined in a nanocage[19] have been studied by the analysis of the ^{1}H spinning sideband (SSB) patterns under magic angle spinning (MAS).

In this study, $^{1}H-^{1}H$ dipolar interactions are utilized to determine the multisite dynamics of form II of *i*PB. It is shown that the complex dynamics of the backbone and the side chains at the fast motional limit effectively suppresses multispin interactions and results in ^{1}H SSB patterns even at slow MAS frequencies. Conventional $^{1}H-^{13}C$ wide line separation (WISE)[13−16] provides averaged dipolar patterns for CH_2 geminal protons of the main and side chains. Specific dynamic geometries and lateral conformations are extracted from the observed dipolar patterns for CH_2 geminal protons under a two-spin approximation.

Theory

Under a two-spin approximation, the dependence of the resonance frequency on the orientation for a homonuclear dipolar interaction is given by

$$\omega(\theta) = \frac{1}{2}\delta[3\cos^2\theta - 1] \quad \text{and} \quad \delta = \frac{3}{2}D_{\mathrm{II}} \tag{1}$$

where δ is the anisotropy parameter, θ is the polar coordinate related the magnetic field, B_0 to the unique axis of dipolar interaction, and D_{II} is homonuclear dipolar coupling constant. $D_{\mathrm{II}}/2\pi$ is 20.6 kHz for CH_2 geminal protons with an internuclear distance of $r_{\mathrm{HH}} = 0.18$ nm. At the fast motion limit ($\tau_c \gg 1/\delta$, where τ_c is correlation time), the angular dependence of the NMR frequency becomes

$$\bar{\omega}(\Theta, \Psi) = \frac{1}{2}\bar{\delta}[3\cos^2\Theta - 1 - \bar{\eta}\sin^2\Theta\cos(2\Psi)] \tag{2}$$

where $\bar{\delta}$ and $\bar{\eta}$ are the averaged anisotropy and averaged asymmetry parameter, respectively, and (Θ, Ψ) are the polar angles of B_0 in the averaged principal axes. $\bar{\delta}$ and $\bar{\eta}$ depend on the dynamic geometry as well as the population of the different sites involved in the dynamic process.[12,20,21]

Experiments

The NMR experiments were performed on a Bruker AVANCE 300 spectrometer equipped with a 7 mm double resonance high-temperature probe. ^{13}C cross-polarization (CP) MAS and ^{1}H MAS SS-NMR spectra were obtained at a MAS frequency of 4 kHz. The phase sensitive $^{1}H-^{13}C$ 2D WISE NMR spectrum was obtained in TPPI mode at a MAS frequency of 6.8 kHz. The data matrix had 512 points along the t_2 dimension

*Corresponding author: e-mail t-miyoshi@aist.go.jp; Tel +81-298-61-9392; Fax +81-29-861-4437.

 Published on Web 03/26/2010

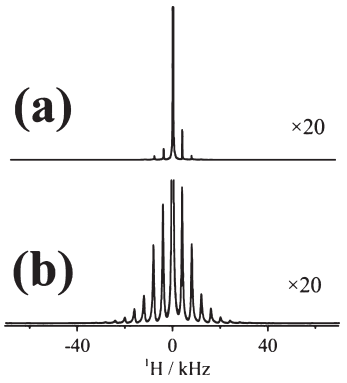

Figure 1. ^{1}H MAS NMR spectra of *i*PB1 in (a) the melt state at 401 K and (b) form II-rich at 373 K at a MAS frequency of 4 kHz.

and 128 points along the t_1 dimension with a dwell time of 7 μs. A short CP of 50 μs was utilized for the polarization transfer step. Continuous wave (CW) decoupling with a field strength of 55 kHz was applied in t_1 dimension to suppress ^{1}H−^{13}C heteronuclear interaction.[14−16] The temperature was calibrated using $Pb(NO_3)_2$.[22] *i*PB1 with a weight-average molecular weight of 185 000 was purchased from Poly Science Co. Ltd. The isotacticity ⟨*mmmm*⟩ was determined to be 92% by solution ^{13}C NMR. The form II-rich sample was prepared by melt crystallization at 373 K for 24 h. The dipolar pattern of two spin pairs under MAS was simulated in the frequency domain by home-written software in Fortran 95.

Results and Discussion

Figure 1a,b shows the ^{1}H MAS spectra of the melt at 401 K and form II rich at 373 K at a MAS frequency of 4 kHz. The melt spectrum is dominated by the isotropic component, with only very minor SSB patterns. This means the motions in the melt are nearly isotropic but cannot completely average out all of the ^{1}H−^{1}H dipolar interactions. On the other hand, the form II-rich spectrum is dominated by intense SSB patterns originating from form II in addition to some contribution from an amorphous state. Very intense SSB patterns reflect a fast but anisotropic complex dynamics in the backbone,[8,9] conformational transitions in the ethyl group,[8] and methyl rotations.[9] The ^{13}C relaxation time, T_1, is sensitive to high-frequency motions with a minimum close to an inverse τ_c of ∼75 MHz, which should result in a T_1 minimum value of ∼0.1 s. The main-chain (m-) CH_2, side-chain (s-) CH_2, and CH have T_1 values of 0.25, 0.32, and 0.38 s, respectively, close to a theoretically minimum value of ∼0.1 s. This simple T_1 result suggests the dynamic frequency for the coupled side group and backbone motions is on the order of ∼10 MHz or higher. Such high-frequency dynamics are normally rare in the solid state, especially in rigid crystalline phases, and are close to the frequency range in the melted state. This may be a specific character of the CONDIS phase. Additionally, parallel packing of stems in the crystalline field inhibits isotropic motions but allows anisotropic motions (the geometry of the stem itself will be discussed later). These structural constraints and fast dynamics in both the side chain and backbone with different dynamic axes effectively decouple the ^{1}H−^{1}H dipolar interactions and result in SSB patterns in the form II spectrum.

The top of Figure 2a shows the ^{13}C CPMAS NMR of form II at 373 K at a MAS frequency of 6.8 kHz. The assignment of the signals is also shown. In a former work,[8] direct polarization (DP) NMR spectra showed very sharp melt-state ^{13}C signals overlapping with the form II signals. Comparison of CP and DP MAS NMR spectra indicates that the CP time of 1 ms in this work excites only the form II signals. At this high temperature, the almost isotropic motions in the amorphous regions do not allow

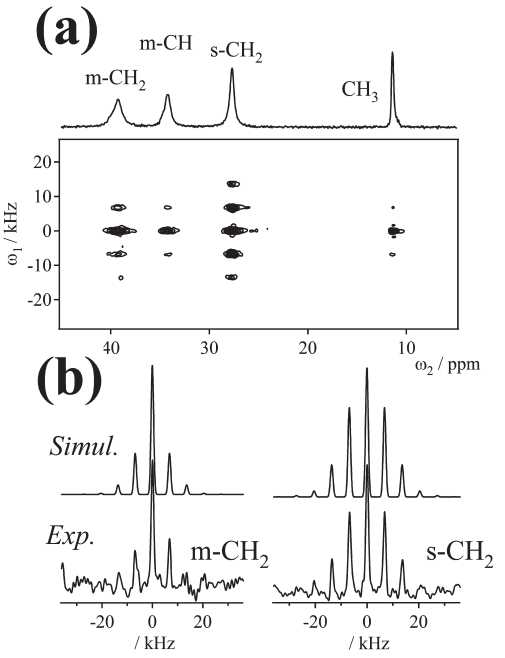

Figure 2. (a) ^{13}C CPMAS NMR spectra of form II with a CP time of 1 ms and the ^{1}H−^{13}C WISE NMR spectrum recorded at 373 K with a CP time of 50 μs under a MAS frequency of 6.8 kHz and TPPM decoupling with a field strength of 65 kHz. CW decoupling with a field strength of 55 kHz in the t_1 dimension was applied to suppress ^{1}H−^{13}C heteronuclear dipolar interactions. (b) The ^{1}H slice and simulated data for s-CH_2 and m-CH_2 geminal protons. The best fitted results show $|\bar{\delta}|/\delta = 0.44 \pm 0.02$ ($D_{II}/2\pi = 9.0 \pm 0.5$ kHz) and 0.61 ± 0.02 (12.5 ± 0.5 kHz) for m-CH_2 and s-CH_2 geminal protons, respectively.

efficient polarization transfer from ^{1}H to ^{13}C. Figure 2a also shows the ^{1}H−^{13}C two-dimensional (2D) WISE spectrum at a MAS frequency of 6.8 kHz at 373 K. Here, a short CP (CP time = 50 μs) was used as a polarization transfer, which does not allow spin diffusions between the different functional groups in the polymers.[15,16] The analysis of the ^{1}H slices provides local ^{1}H−^{1}H dipolar interactions for each functional group. ^{1}H slices for s-CH_2 and m-CH_2 geminal protons are shown in Figure 2b. For both ^{1}H slices, the line widths of the SSB signals at *n* order show almost same with the center line at $n = 0$, where *n* is an integer. Schnell et al. simulated third spin effects on the ^{1}H SSB signals at *n* order depending on geometry and distances.[18] They realized that if a third spin significantly interacts with the isolated spin pairs, asymmetric line shapes shall appear, depending on the relative geometry, the mutual distances of three spins, and the MAS frequency. Our experimental data, however, indicate that all SSB signals at *n* order are symmetric and have similar line widths as the center band. Thus, it can be safely assumed that the two-spin approximation holds for CH_2 geminal protons. Under the two-spin approximation, the dipolar patterns were calculated under an assumption of $\bar{\eta} = 0$. The calculated results reproduce the experimental data very well. Surprisingly, the s-CH_2 geminal protons show much larger $|\bar{\delta}|/\delta = 0.61 \pm 0.02$ ($D_{II}/2\pi = 12.5 \pm 0.5$ kHz) than 0.44 ± 0.02 for m-CH_2 ($D_{II}/2\pi = 9.0 \pm 0.5$ kHz). These results were unexpected in the dynamics of the polymer with a side chain, since side-chain protons are influenced by the complex dynamics of both the main and side chains. Generally, two independent dynamic processes with different dynamic axes result in a smaller dipolar coupling constant in the side groups than that in the main chains. In fact, Mirau et al. detected smaller line widths for the side group than that in main chain of poly(ethyl methacrylate) (PEMA) well above T_g.[16] The experimental results presented here are

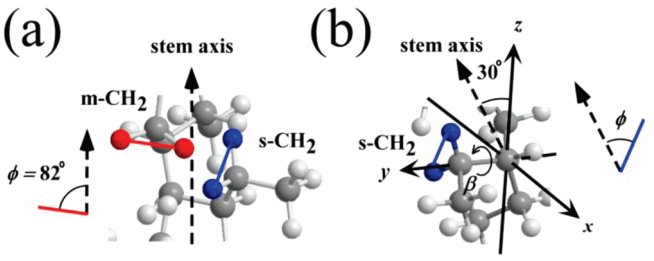

Figure 3. (a) A part of uniform 11_3 helical stem of form II of *i*PB1 assuming *trans*−*gauche*′ conformation ($\beta = 60°$) in the side chain. Dipolar vectors of m- and s-CH_2 protons being colored by red and blue, respectively. (b) Expanded side-chain structure in the new frame whose *y* axis being set to s-CH_2−CH carbon bond (rotation axis). The stem axis in the *yz* plane is inclined to the *z* axis in this frame by an angle of 30°.

opposite to those expected in the side-chain polymers but shall be explained by the assumption of an anisotropic dynamical process as shown below.

The effects of the dynamic geometry of overall and side chains on the ^{1}H SSB patterns were considered next. In the crystalline region, parallel packing of the stems restricts the overall dynamics to uniaxial motions around the stem axes. For several CONDIS crystals such as PE in the hexagonal phase,[3] 1,4-*trans*-polybutadiene in the high-temperature phase,[23] and PDES,[12] it has been reported by SS-NMR that stems commonly show uniaxial diffusions around the axes. Under such conditions, $\bar{\eta}$ is 0 and $|\bar{\delta}|$ is described in terms of a following equation:

$$|\bar{\delta}| = \frac{1}{2}\,\delta|3\cos^2\phi - 1| \tag{3}$$

where ϕ is an angle between dipolar vector of the germinal protons and dynamic axis.[24] Figure 3a shows a relationship between dipolar vectors and stem axis assuming uniform 11_3 helix with the side chain adopting the *trans*−*gauche*′ conformation with a dihedral angle, β, of 60°. The dipolar vector of m-CH_2 is inclined by an angle of 82° with respect to the stem axis. Thus, $|\bar{\delta}|/\delta$ for m-CH_2 geminal protons at a fast uniaxial diffusion is calculated to be 0.47 using the above equation. This value is consistent with the experimentally obtained value of 0.44 ± 0.02. The small reduction in the observed value may be due to small librations around the C−C bonds of main chains and/or slight conformational deviations from an ideal 11_3 helix.

The $|\bar{\delta}|/\delta$ value for the s-CH_2 geminal protons (0.61 ± 0.02) is the result of the complex dynamics of the fast spinning backbone and conformational transitions of the side chain. The overall dynamic effect of s-CH_2 protons in different conformations with a dihedral angle, β, on the dipolar pattern and the conformational jump effect as a function of jump angle, α, were examined further. It is noted that the jump angle α corresponds to a difference between dihedral angles in two interchanging conformations, $|\beta_1 - \beta_2|$, where 1 and 2 denote two conformations.

First, we treat the β dependence of the dipolar patterns of s-CH_2 protons under overall dynamics. To clarify the relationship between β and ϕ, another coordinate frame was established as shown in Figure 3b. Here, s-CH_2−CH carbon bond which is the rotation axis for side-chain conformation is aligned along *y* axis. The vector of s-CH_2 germinal protons is orthogonal to the rotation axis. In this frame, the stem axis is tilted in the *yz* plane and makes an angle of 30° with *z* axis. Thus, the angle ϕ between the stem axis and dipolar vector of s-CH_2 protons has the following relation with β:

$$\cos\phi = \cos(30)r_{CH}\sin\gamma(\cos(\beta - 58) - \cos(\beta + 62))/r_{HH} \tag{4}$$

where r_{CH} is a C−H distance (0.11 nm) and γ is an angle between CH vector and *y* axis (71°). Using eqs 3 and 4, the β dependence of

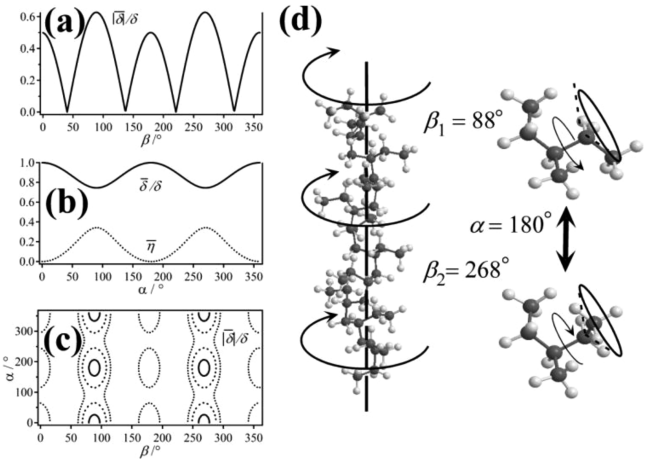

Figure 4. (a) Uniaxially overall diffusion effect on $|\bar{\delta}|/\delta$ for s-CH_2 geminal protons as a function of a dihedral angle, β. (b) Conformational transition effect on $\bar{\delta}/\delta$ (solid line) and $\bar{\eta}$ (dotted line) for s-CH_2 geminal protons as a function of the jump angle α. (c) Both dynamics effects on $|\bar{\delta}|/\delta$ (solid ($|\bar{\delta}|/\delta = 0.6$), dashed (0.5), and dotted (0.4) lines) for s-CH_2 geminal protons as functions of β and α. (d) Molecular dynamics of form II determined by ^{1}H dipolar patterns.

$|\bar{\delta}|/\delta$ for the s-CH_2 geminal protons due to the overall dynamics is shown in Figure 4a. The $|\bar{\delta}|/\delta$ value dramatically changes depending on β. These overall dynamics effectively average out dipolar interaction between s-CH_2 protons. It is found that only the conformations at $\beta = 88$ or $268 \pm 10°$ satisfy the experimental value of $|\bar{\delta}|/\delta = 0.61 \pm 0.02$. The other conformations result in much smaller $|\bar{\delta}|/\delta$ values. In fact, the two conformations with $\beta = 60°$ and 300° obtained by MM3 calculation and high-resolution NMR give about half the value of the experimental result, $|\bar{\delta}|/\delta = 0.37$ and 0.33, respectively.

In addition, two-site jump motions due to a conformational transition also reduce the dipolar interaction and can be analyzed to give solutions for different populations in the two sites.[12,20,21] The population ratios of 78 and 22 for two conformations were applied at $\beta_1 = 60°$ and $\beta_2 = 300°$, respectively, obtained in the former SS-NMR work.[8] Then, $\bar{\delta}$ and $\bar{\eta}$ are described by a function of the jump angle, α, as follows:

$$\bar{\delta} = \delta\left(\frac{1}{4} + \frac{3}{4}\sqrt{\cos^2\alpha + 0.44\sin^2\alpha}\right) \quad \text{and}$$

$$\bar{\eta} = \frac{3\left(1 - \sqrt{\cos^2\alpha + 0.44\sin^2\alpha}\right)}{\left(1 + 3\sqrt{\cos^2\alpha + 0.44\sin^2\alpha}\right)} \tag{5}$$

Figure 4b shows effects of the side-chain dynamics on $\bar{\eta}$ and $\bar{\delta}/\delta$ as a function of α. $\bar{\delta}/\delta$ leads to a minimum value of 0.75 at $\alpha = 90°$ and goes to a maximum of 1.0 at $\alpha = 0$ and 180°. The conformational transition at $\alpha = 180°$ can no longer change dipolar interactions for the isolated two spins. However, this transition effectively averages out the higher spin interactions. $\bar{\eta}$ also strongly depends on α. Figure 4b shows that $\bar{\eta}$ is 0 only for $\alpha = 0$ and 180°. Actually, overall and side-chain dynamics are present in form II, and both effects on $|\bar{\delta}|/\delta$ are shown in Figure 4c. The $|\bar{\delta}|/\delta$ value of 0.6 is shown as a solid curve. Two independent dynamics severely limit possible conditions at $\beta = 88°$ and $268 \pm 10°$ and their transitions with $\alpha = 180 \pm 20°$ or no dynamics ($0 \pm 20°$) which satisfy the experimental $|\bar{\delta}|/\delta$ value. These conditions also satisfy $\bar{\eta} = 0$. However, the lack of lateral dynamics does not average out higher spin interactions within the stem. Thus, this possibility is unlikely. Therefore, it is concluded that form II of *i*PB1 performs uniaxial diffusions accompanying the conformational transition ($\alpha = 180 \pm 20°$) of the side chain

between two conformations at $\beta = 88$ and $268 \pm 10°$ in the fast-motional limit (Figure 4d).

Summary

The complex dynamics of the backbone and side chains of form II of *i*PB1 were investigated in terms of $^1H-^1H$ dipolar patterns of the CH_2 geminal protons under a two-spin approximation. The observed dipolar patterns were successfully analyzed in terms of complex dynamics of uniaxial overall diffusions and conformational transitions of the side chain between the conformations at dihedral angles of $\beta = 88°$ and $268 \pm 10°$. Such unique dynamics in both side and main chains are unlikely in the crystalline phase[25,26] but may be typical in the disordered phase.[3,4] Additionally, fast dynamics as found here were observed in polymers confined in a nanospace.[4,27] Conventional $^1H-^{13}C$ WISE NMR can offer the unique opportunity for unraveling multisite dynamics of polymers confined in a nanospace without isotope labeling.

References and Notes

(1) Wunderlich, B.; Moller, B.; Grebowicz, J.; Baur, H. *Adv. Polym. Sci.* **1988**, *87*, 1.
(2) Ungar, G. *Polymer* **1993**, *34*, 2050–2059.
(3) Allegra, G.; Meile, S. V. *Macromolecules* **2004**, *37*, 3487–3496.
(4) Sozzani, P.; Bracco, S.; Comotti, A.; Simonutti, R. *Adv. Polym. Sci.* **2005**, *181*, 153–177.
(5) Hu, W.-G.; Shimidt-Rohr, K. *Acta Polym.* **1999**, *50*, 271–285.
(6) Luciani, L.; Seppälä, J.; Löfgren, B. *Prog. Polym. Sci.* **1988**, *13*, 37–62.
(7) Petraccone, V.; Pirozzi, B.; Frasci, A.; Corradini, P. *Eur. Polym. J.* **1976**, *12*, 323–327.
(8) Miyoshi, T.; Hayashi, S.; Imashiro, F.; Kaito, A. *Macromolecules* **2002**, *35*, 6060–6063.
(9) Zemke, K.; Schmidt-Rohr, K.; Spiess, H. W. *Acta Polym.* **1994**, *45*, 148–159.
(10) Allinger, N. L.; Yuh, Y. H.; Lii, J. H. *J. Am. Chem. Soc.* **1989**, *111*, 8551–8566.
(11) Maring, D.; Whilhelm, M.; Spiess, H. W.; Meurer, B.; Weill, G. *J. Polym. Sci., Part B: Polym. Phys.* **2000**, *38*, 2611–2624.
(12) Litvinov, V. M.; Macho, V.; Spiess, H. W. *Acta Polym.* **1997**, *48*, 471–477.
(13) Schmidt-Rohr, K.; Clauss, J.; Spiess, H. W. *Macromolecules* **1992**, *25*, 3273–3277.
(14) Tekely, P.; Palmas, P.; Mutzenhardt, P. *Macromolecules* **1992**, *26*, 7363–7365.
(15) Palmas, P.; Tekely, P.; Canet, D. *Solid State Nucl. Magn. Reson.* **1995**, *4*, 105–111.
(16) Qiu, X.; Mirau, A. P. *J. Magn. Reson.* **2000**, *142*, 183–189.
(17) Forbes, J.; Husted, C.; Oldfield, E. *J. Am. Chem. Soc.* **1988**, *110*, 1059–1065.
(18) Schnell, I.; Spiess, H. W. *J. Magn. Reson.* **2001**, *151*, 153–227.
(19) Sekine, S.; Kubo, A.; Sano, H. *Chem. Phys. Lett.* **1990**, *171*, 155–160.
(20) Schmidt-Rohr, K.; Spiess, H. W. *Multidimensional Solid-State NMR and Polymers*; Academic Press: London, 1994.
(21) Reichert, D.; Schneider, H. *Z. Phys. Chem.* (*Munich*) **1995**, *190*, 63–71.
(22) Bielecki, A.; Burum, D. P. *J. Magn. Reson. A* **1995**, *116*, 215–220.
(23) Möller, M. *Macromol. Chem., Rapid Commun.* **1988**, *9*, 107–114.
(24) Abragam, A. *The Principle of Nuclear Magnetism*; Oxford University Press: London, 1961.
(25) Miyoshi, T.; Pascui, O.; Reichert, D. *Macromolecules* **2004**, *37*, 6460–6471.
(26) Miyoshi, T.; Pascui, O.; Reichert, D. *Macromolecules* **2004**, *37*, 6653–6656.
(27) Uemura, T.; Horike, S.; Kitagawa, K.; Mizuno, M.; Endo, K.; Bracco, K.; Comotti, A.; Sozzani, P.; Nagaoka, M.; Kitagawa, S. *J. Am. Chem. Soc.* **2008**, *138*, 6781–6788.